Journal of Transportation Engineering, Vol.127, 357-362 (2001)

REFINEMENT OF THE SUPERPAVE SPECIFICATION PARAMETER FOR PERFORMANCE GRADING OF ASPHALT

AROON SHENOY

Senior Research Fellow

Turner-Fairbank Highway Research Center

6300 Georgetown Pike

McLean, VA 22101

Tel: (202) 493 3105

Fax: (202) 493 3161

E-mail: aroon.shenoy@fhwa.dot.gov

]

Abstract

The Superpave specification parameter $|G^*|/\sin\delta$ for high temperature performance grading of paving asphalts has not been found to be adequate in rating various binders, especially some polymer-modified ones, for their rutting resistance. This has led researchers to seek other possible parameters that may better relate to rutting resistance and also to search for ways to improve the existing parameter $|G^*|/\sin\delta$ so that it is more sensitive to pavement performance. Some researchers have suggested the repeated creep and recovery test, while others have used a semi-empirical approach as a means to refine the existing Superpave specification parameter.

The present work revisits the proposed refinements of the Superpave specification parameter and shows that the semi-empirical approach involving curve-fitting of experimental data is not necessary if the derivations are based on fundamental concepts. The final equations obtained through a theoretical development are verified using part of the same experimental data that were used by the earlier researchers.

Keywords: Superpave specification parameter, repeated creep, creep recovery, rutting resistance, asphalt rheology

INTRODUCTION

The ineffectiveness of the Superpave specification parameter $|G^*|/\sin\delta$ in capturing the high temperature performance of paving asphalts for rating their rutting resistance is a significant concern [Phillips and Robertus, 1996; Stuart and Mogawer, 1997; Bahia et al., 1999; Desmazes et al., 2000; Bouldin et al., 2000, 2001]. The failure of this parameter has been demonstrated through field data during the Accelerated Loading Facility (ALF) testing at the Turner-Fairbank Highway Research Center by Stuart and Mogawer (1997) and also through laboratory testing during the National Co-operative Highway Research Program (NCHRP) Project 9-10 by Bahia et al. (1999).

Repeated creep and recovery test for binders (RCRB) is being suggested (Bahia et al., 1999) as a possible means to estimate the rate of accumulation of permanent strain in the binders. The RCRB test protocol consists of applying a creep load of 0.3 kPa for a 1-second duration (loading time) followed by a 9-second recovery period (rest period) for 100 cycles.

Bouldin et al. (2000, 2001) have utilized the RCRB as proposed by Bahia et al. (1999) to evaluate the relative rut resistance of test binders. The generated experimental data were then used by Bouldin et al. (2001) to develop a semi-empirical model to refine the current Superpave high temperature specification parameter $|G^*|/\sin\delta$.

In revising the Superpave high temperature specification, Bouldin et al. (2001) state that one of the following three options could be used:

- Perform RCRB at the high specification temperature using an appropriate loading rate and then use the measured accumulated strain after N number of cycles as the specification criterion
- Fit the individual repeated creep curves numerically to a phenomenological model and use the model curve-fitting parameters to rank the binders as per the suggestion of Bahia et al. (1999)
- Develop a semi-empirical model that fits the RCRB results through data generated from the conventional frequency sweep tests from the Dynamic Shear Rheometer (DSR)

Bouldin et al. (2001) preferred to use the third option of a semi-empirical approach as they believed that it would better account for the increased influence of the phase angle δ on the accumulated strain. They designated accumulated strain as γ_{acc}, though they actually use the strain that is unrecovered after one cycle of a creep test. Hence, in the present paper, their nomenclature is changed to γ_{unr}, which represents the unrecovered strain after one cycle. It would be more appropriate to use γ_{acc} to designate the accumulated strain after N cycles.

Their approach is based on the assumption that the strain accumulation rate depends upon the binder stiffness and the viscoelasticity contribution $f(\delta)$ (at the appropriate rate and temperature) and that these two contributions are independent. The equation for the rutting resistance is thus (Bouldin et al., 2001):

$$R = \%\gamma_{unr}^{-1} = G^{*}.\, f(\delta) - (1)$$

The binder stiffness was shown to be related to the maximum strain per cycle through the following equation, which fitted with an R^2 = 0.996 for equation (2a) and R^2 = 0.93 for equation (2b):

$$\%\gamma_{\max} = \frac{2.6}{G^{*1.15}} - (2a)$$

$$\%\gamma_{\max} = \frac{2.4}{G^{*1.17}} - (2b)$$

where the binder stiffness G* is expressed in kPa.

Using a truncated Taylor series, Bouldin et al. (2000) suggested the following expression for the unrecovered strain:

$$\%\gamma_{unr}^{-1} = G^{*}.\left\{k_1 \sin^{-1}\delta + k_2 \sin^{-2}\delta\right\} - - - - - - - - - - - - - - - - - (3a)$$

where k_1 and k_2 are empirical constants. They stated that, as more performance data becomes available and analyzed, the values of the empirical constants could be more accurately determined. On analyzing more data on different binders, a different functional form was suggested in the subsequent work by Bouldin et al. (2001).

Bouldin et al. (2001) plotted the ratio of the unrecovered strain to the maximum strain $\gamma_{unr}/\gamma_{max}$ versus the phase angle to find the function f (δ). The best fit of the experimental data based on the evaluated binders was obtained through the empirically determined hyperbolic function to give the following expression for the unrecovered strain:

$$\%\gamma_{unr}^{-1} = k.G^{*}.\left\{Y_0 + a\left[1 - 1/\exp\left[\left(\left|\left(\delta - X_0 + b\ln(2)^{1/c}\right)\right|/b\right)^{c}\right]\right]\right\} - - (3b)$$

where k is a constant and Y_0, X_0, a, b, and c are empirical fitting parameters. It has been shown by Bouldin et al. (2001) that the measured unrecovered strain from the RCRB is well predicted by this empirical equation (3b) with an R^2 of 0.942.

Bouldin et al. (2001) proposed refinement of the Superpave specification parameter involves five empirical fitting parameters. The values of the five empirical fitting parameters are likely to change if more data are analyzed, or if experimental data of the replicates are used instead of those on the original samples. In other words, equation (3b), which was obtained by curve-fitting experimental data, cannot be truly treated as a general equation that would be applicable at all times.

In the present paper, it will be shown that it is possible to provide a refinement to the Superpave high temperature specification parameter by following basic principles and deriving the methodology through fundamental concepts rather than by curve-fitting experimental data. It will be seen that the controlling equations evolve through a systematic derivation and not by curve-fitting. The experimental data are used not for extracting a correlation but only to confirm that the theoretical derivation is sound.

THEORETICAL DEVELOPMENT

The first step is to understand what actually happens during the repeated creep recovery test. On applying a stress of σ_0 kPa for duration of 't' seconds, the total deformation (or the maximum strain (γ_{max}) that the material undergoes must be the sum of the elastic deformation and the viscous deformation. From basic principles, the deformation behavior has to be mapped by the following equation relating the applied constant stress with the maximum strain:

$$\%\gamma_{max} = \frac{100\sigma_0}{|G^*|} \quad \text{----------} \quad (4)$$

where σ_0 is the applied stress (kPa) in the creep experiment and |G*| is the complex modulus (kPa) obtained from oscillatory shear at matching time scale. Substituting σ_0 = 0.3 kPa as used by Bouldin et al. (2000, 2001) during their creep experiment in the above equation (4) gives the following simple relationship:

$$\%\gamma_{max} = \frac{30}{|G^*|} \quad \text{----------} \quad (5)$$

In the expressions obtained by Bouldin et al. (2000, 2001), as shown in equations (2a) and (2b), neither the coefficient nor the power matches that of equation (5).

The discrepancy arises from the fact that in arriving at equations (2a) and (2b), the time scales were not matched. The strain $\%\varepsilon_{max}$ represents the value from the creep experiment while the stiffness |G*| that is used in equation (2) is obtained from the frequency sweep oscillatory measurement. To obtain a relationship between the two, comparisons must be made on a common platform, thereby requiring the time scales to be matched. If the loading in the creep experiment is 1 second, then the |G*| value at oscillation frequency ω = 1 radians/s must be used; whereas, if the loading in the creep experiment is 10 seconds, then the |G*| value at ω = 0.1 radians/s must be used to match the time scale.

Bouldin et al. (2000, 2001) used $\%\varepsilon_{max}$ values for a creep experiment loading duration of 1 second and compared them with |G*| values for ω = 10 radians/s. This mismatch of time scales leads to the values of coefficient and power in equation (2), which are different from those in equation (5). The major advantage of using matched time scales is that the significance behind the relationship between $\%\varepsilon_{max}$ values from a creep experiment with |G*| values from a frequency sweep during oscillatory shear experiments becomes apparent. Hence, equation (5) should be the preferred method of seeking a relationship between the $\%\varepsilon_{max}$ from a creep experiment and |G*| from a frequency sweep during an oscillatory shear experiment.

Having obtained the simple expression for the maximum strain per cycle from a creep loading experiment through basic principles, the next step is to focus on the recovery part of the creep experiment. In the linear range of response, under constant stress, the strain per unit stress is a unique function of time t referred to as the shear creep compliance function (Plazek and Frund, 2000), which can be described by the following equation:

$$J(t) = J_e + J_d\psi(t) + \frac{t}{\eta} = \frac{\%\gamma(t)}{100\sigma_0} \quad \text{----------(6)}$$

where J(t) is the shear creep compliance; J_e is the elastic recoverable shear compliance; J_d is the delayed recoverable shear compliance; ψ(t) is the normalized retardation function which ranges from zero at t=0 to one when steady-state deformation is achieved; η is the steady-state viscosity; and t/η is the contribution of the viscous deformation at time t that is unrecoverable.

The recoverable shear compliance $J_r(t)$, which can be measured directly from the recoverable deformation following the cessation of creep loading, is given by:

$$J_r(t) = J_e + J_d y(t) \quad \text{----------} \quad (7)$$

If it is assumed that sufficient time has elapsed for asymptotic conditions to be reached, then the steady-state recoverable creep compliance J_{rec} can be written as:

$$J_{rec} = J_e + J_d \quad \text{----------} \quad (8)$$

It can be shown from continuum mechanics and experiments (Bird et al., 1977) that the steady-state recoverable creep compliance is related to the steady shear flow property as follows:

$$J_{rec} = \lim_{\dot{g} \to 0} J(\dot{g}) = \frac{t_{11} - t_{22}}{2t_{12}^{\ 2}} \quad \text{----------} \quad (9)$$

where J_{11} - J_{22} is the normal stress difference and J_{12} is the shear stress. It has been shown in Shenoy and Saini (1996) that the following relationships hold based on the Spriggs model:

$$t_{11} - t_{22} = 2C^{-2}G' \qquad forw = C\dot{g} \quad \text{----------} \quad (10)$$

and

$$t_{12} = C^{-1}G'' \qquad forw = C\dot{g} \quad \text{----------} \quad (11)$$

where GN is the storage modulus, G0 is the loss modulus, and C is an arbitrary adjustable constant. When C = 1, the model suggests an association between steady and dynamic shear data at an equivalent shear rate and frequency. It may be noted that the value of C truly does not matter as it cancels out in the ratio, when equations (9) - (11) are combined. During creep recovery after the removal of the applied stress, the strain rates are very low and hence, the comparison is made in the low shear rate / low frequency regimes. In the limit of shear rates tending to zero, or in other words, in the low shear rate / low frequency regions, the relationship given by equation (9) can be rewritten as follows:

$$J_{rec} = \frac{G'}{G''^2} \text{ - (12)}$$

or from the definition of J_{rec}, can be written as:

$$\frac{\%\gamma_{rec}}{100\sigma_0} = \frac{G'}{G''^2} \text{ - (13)}$$

If sufficient time is given for the creep recovery, it is clear that all the elastic strain is recovered and the viscous strain is left unrecovered. It is often believed that the delayed elastic portion of the strain leaves remnants of the elastic strain, which then adds to the viscous strain if sufficient time for recovery has not elapsed.

In the RCRB experiments performed by Bahia et al. (1999) and Bouldin et al. (2000, 2001), observations are that the delayed elastic strain is completely recovered. First, the creep recovery time is approximately10 times the creep loading time; second, recovery times of 9 seconds and 90 seconds are likely to be greater than the relaxation time of the binder, especially because the temperatures of measurement are at and around the high specification temperature; third, and most importantly, the observed curve after repeated loading is a simple straight line. If the elastic recovery is not complete, then every subsequent cycle would have its peak value decreasing (slowly but surely) and its unrecoverable strain value decreasing (again slowly but surely), thereby showing nonlinear behavior. Since the line joining the unrecoverable strain after every cycle is nearly a straight line in almost all cases that were tested (Bouldin et al., 2001), there is good evidence to suggest that the delayed elastic strain effect is minimal. In fact, Bahia et al. (1999) state that in all of their observations the delayed elastic strain constituted less than 2% of the total strain. Nevertheless, the contribution of the delayed elastic strain effect must be taken into account if the intention is to develop a general relationship for viscoelastic systems, such that the derived expressions would be valid in situations when the recovery times are shorter or the temperatures of measurement are lower.

The percent recoverable strain can be written as:

$$\%\gamma_{rec} = \%\gamma_{\max} - \%\gamma_{unr} \text{ - - - - - - - - - - - - - - - (14)}$$

Combining equation (4), (13), and (14), the following equation is written with a rearrangement of the terms as:

$$\frac{\%g_{unr}}{\%g_{\max}} = 1 - \frac{|G^*|G'}{G''^2} \text{ - - - - - - - - - - - - - - - - (15)}$$

Using the fact that G = |G*|cosδ and G = |G*|sinδ, equation (15) can be simplified as:

$$\frac{\%g_{unr}}{\%g_{\max}} = 1 - \frac{1}{\tan d \sin d} \text{ - - - - - - - - - - - - - - - (16)}$$

Equation (16) provides the refinement of the Superpave specification parameter. The current specification parameter is derived directly through the definition of the loss compliance as follows:

$$\frac{\%g_{unr}}{100s_0} = J'' = |J^*|\sin d = \frac{\sin d}{|G^*|} \text{ - - - - - - - - - - - - (17)}$$

Thus, combining equation (17) with equation (4) gives the equivalent of equation (16) based on the current specification parameter.

$$\frac{\%g_{unr}}{\%g_{\max}} = \sin d \text{ - (18)}$$

Equation (16) gives a value of $\%(_{unr}/\%(_{max}$ that is equal to1 when the phase angle * is 90 degrees. However, the form of the equation does not allow its use to values below * = 52 degrees, because it would then predict unrealistic negative values of $\%(_{unr}/\%(_{max}$. The values of * < 52 degrees may be obtained at low or moderate test temperatures, but the focus of the present work is limited to the high temperature range. It can be seen from Bouldin et al. (2001) that for a large number of the systems that they analyzed, the validity of equation (16) between * = 52 and 90 degrees would be sufficient to encompass most binder data in the high specification temperature regime.

Substituting equation (4) in equation (16) gives the expression for % unrecovered strain as:

$$\%g_{unr} = \frac{100s_0}{|G^*|}\left(1 - \frac{1}{\tan d \sin d}\right) \text{ - - - - - - - - (19)}$$

Since |G*| and * are functions of frequency and temperature, the effect of traffic speed and pavement temperature are built into this equation. To minimize the unrecovered (or permanent) strain, the following term needs to be maximized:

$$\frac{|G^*|}{\left(1-\frac{1}{\tan d \sin d}\right)} \text{ - - - - - - - - - - - - - - - - - (20)}$$

Equation (20) would then be the new specification parameter, replacing |G*|/sin*. The high specification temperature can now be specified as the temperature at which the term given by equation (20) takes a value of 1 kPa for the original unaged binder and a value of 2.2 kPa for the RTFOT aged binder. The values of 1 kPa for the original unaged binder and 2.2 kPa for the RTFOT aged binder have been retained because only then the equation predicts the same specification temperatures for unmodified binders as predicted under the earlier Superpave specification system. Any new specification parameter or its refinement should maintain the specification value for unmodified binders while providing a better means of specification for modified binders.

As an alternative, the new specification parameter could be based on the value of * alone. This is possible on account of the form of the expression given by equation (19). It can be seen that equation (19) predicts that the $\%(_{unr}$ is zero at conditions when the following equality holds:

$$\tan d \sin d = 1 \text{ - - - - - - - - - - - - - - - - - (21)}$$

or

$$d(w_{spec}, T_{hi,spec}) \approx 52(\deg rees) \text{ - - - - - - - - (22)}$$

Equation (22) implies that the temperature at which the phase angle equals to 52 degrees at a particular predecided frequency (for example, ω_{spec} =1 radians/s or ω_{spec}=10 radians/s) could be used as the new specification parameter $T_{hi,spec}$. This would ensure that the unrecovered strain is minimal or close to zero at conditions of temperature < $T_{hi,spec}$ and frequency of loading > ω_{spec}. The possible disadvantage of using equation (22) in preference to the parameter given by equation (20) is that there are chances of offsetting the cost-benefit ratios in choosing materials and coming up with highly conservative choices.

EXPERIMENTAL VERIFICATION

The theoretical development in the previous section has shown that the refinement to the Superpave specification temperature can be derived from basic principles. Verification of the obtained relationships is necessary. Experimental data on some typical asphalts that have widely different rheological characteristics are used for verification. The data used for verification are part of the same data that were used by Bouldin et al. (2001) in their work.

The experiments performed were creep (followed by recovery) and the frequency sweep on the dynamic shear rheometer (DSR) at different temperatures for each asphalt sample. The creep experiments were performed under a fixed imposed stress F_0 of 0.3 kPa while (a) using 1-second loading time followed by a 9-second recovery time in most cases and (b) using 10-second loading time followed by a 90-second recovery time in some cases.

The frequency sweep data were generated using a set of parallel plates of 25- mm diameter following the procedure given in the AASHTO provisional specifications (AASHTO 2000). The samples for the test were prefabricated using a silicone rubber mold. The data were generated for a frequency range from 0.1 radians/s to 100 radians/s. It was made certain that all generated data were within the linear viscoelastic range of response.

Materials Used

Only a few asphalts at selected temperatures were chosen from among those that were analyzed by Bouldin et al. (2001) for verification of the equations developed in the present analysis. The data set, which covers a temperature range from 46-80^{0}C and phase angle δ from 55-88 degrees, is shown in Table 1. Using this partial data set, the theoretical equations derived from basic principles are verified.

TABLE 1: **Details of the Experimental Data used for Verification of the Theoretical Predictions**

		Creep Recovery Data			Frequency Sweep Data		
Binder	Temp. ^0C	Stress duration seconds	γ_{max} %	γ_{unr} %	ω rad/s	$\|G^*\|$ kPa	δ deg
Styrelf -PMA							
	60.7	10	21.9	6.3	0.1	1.17	58.5
	73.6	10	128.0	70.2	0.1	0.29	66.7
	79.8	10	189.0	116.0	0.1	0.16	71.0
	58.0	1	3.9	0.9	1	6.82	55.2
	70.0	1	11.9	2.9	1	2.16	58.3
	76.0	1	20.2	5.7	1	1.17	60.8
Cariphalte DM							
	79.8	1	61.3	31.4	1	0.60	55.2
PetroCan-PG70-20-Oxd.							
	59.0	1	10.0	4.8	1	4.31	58.3
BP-2-50 Pen							
	73.6	1	147.0	145.0	1	0.21	87.9
821-EVA modified							
	46.6	1	15.6	7.3	1	2.47	72.4

In order to establish authenticity, the best fit curve through the complete data set of Bouldin et al. (2001) on a variety of asphalts as shown in Table 2 is compared with predictions from equation (16).

TABLE 2: **Asphalt Binders evaluated by Bouldin et al. (2001); Data used for obtaining Eq. (25)**

Asphalt Binder	Information on Performance History
AC-5-Conventional	From ALF
AC-10-Conventional	From ALF
AC-20-Conventional	From ALF
Styrelf-PMA	From ALF
PG64-22-Conventional	Nevada D.O.T
AC20P-PMA	Nevada D.O.T
Cariphalte DM-PMA	Anecdotal in Europe
Black Max-PMA	Anecdotal in Canada
Husky(200/300)-Conventional	Anecdotal in Canada
RedWater-200/300-Conventional	N/A
MS-1-ASR-AC6-m	Field Rut Depth
MS-1-GSR-AC11-m	Field Rut Depth
MS-1-RSR-AC10-m	Field Rut Depth
MS-1-TSR-AC4-m	Field Rut Depth
MS-1-PSR-AC5-m	Field Rut Depth
MS-1-CSR-AC11-m	Field Rut Depth
AI-1-76-22-96095	Laboratory Mix Data
AI-2-Conoco-76-2-96-119	Laboratory Mix Data
AI-3-Koch-76-22-96125	Laboratory Mix Data
AI-4-Koch-76-22-96126	Laboratory Mix Data
AI-5-Ashland-76-22	Laboratory Mix Data
Trumbull PG 70-28-Oxd.	Anecdotal
PetroCan-PG70-22-Oxd.	Anecdotal
BP-1-PMB4	Lab Data-Mix & Wheel Tracking (WT)
BP-2-50 Pen	Lab Data-Mix & Wheel Tracking (WT)
BP-3-35 Pen	Lab Data-Mix & Wheel Tracking (WT)
BP-4-Wax3	Lab Data-Mix & Wheel Tracking (WT)
BP-5-PMB5	Lab Data-Mix & Wheel Tracking (WT)
821-EVA modified	Anecdotal

RESULTS AND DISCUSSION

Figure 1 shows a plot of the percent total strain for an applied stress of 0.3 kPa during creep loading versus the complex shear modulus |G*| obtained from the frequency sweep. If the creep loading was for a duration of 1 second, then the value of |G*| at $\omega = 1$ radians/s was used and if the creep loading was for a duration of 10 seconds, then the value of |G*| at $\omega = 0.1$ radians/s was used. It was important to make sure that the value of |G*| was at the same temperature as the temperature of measurement during the creep cycle. This is essential since œomparisons between the results of the two experiments must be made on a common platform.

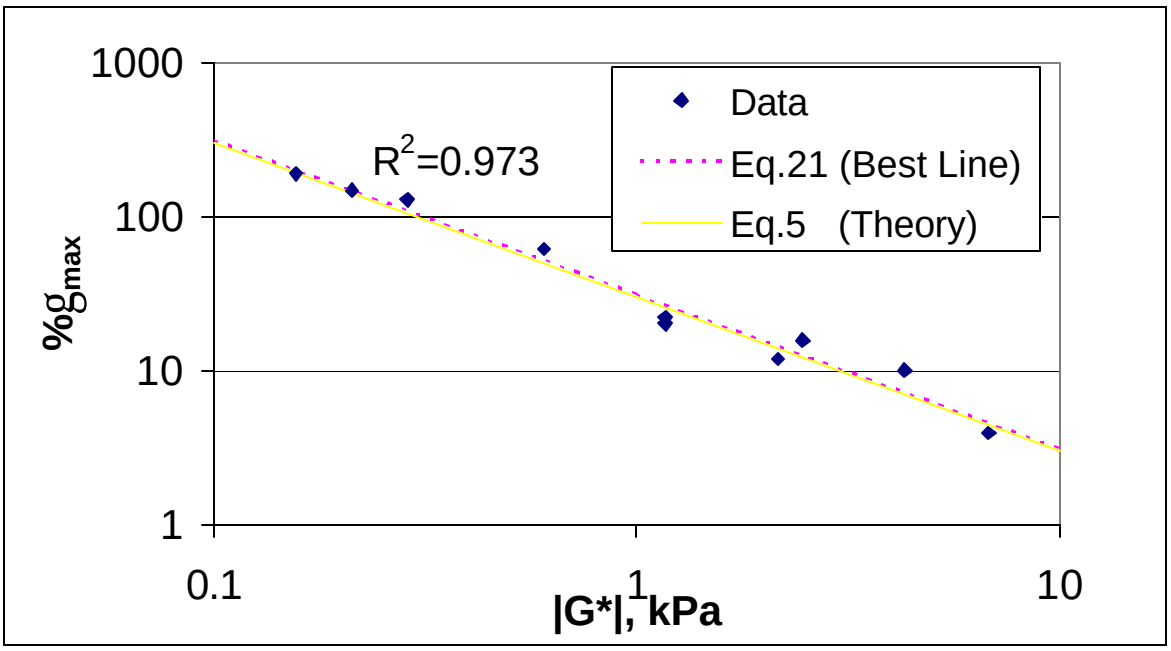

Figure 1: Plot of the percent total strain for an applied stress of 0.3 kPa during creep loading versus the complex shear modulus |G*| obtained from the frequency sweep at matching time scales and temperature.

It was found that the best line through the data points could be fitted with the following equation, which has an R^2 of 0.973:

$$\%g_{max} = \frac{31}{|G^*|} \quad (23)$$

The above equation can be seen to closely match equation (5). In fact, in Figure 1 the solid line that is shown for equation (5) closely follows the dashed line for equation (23).

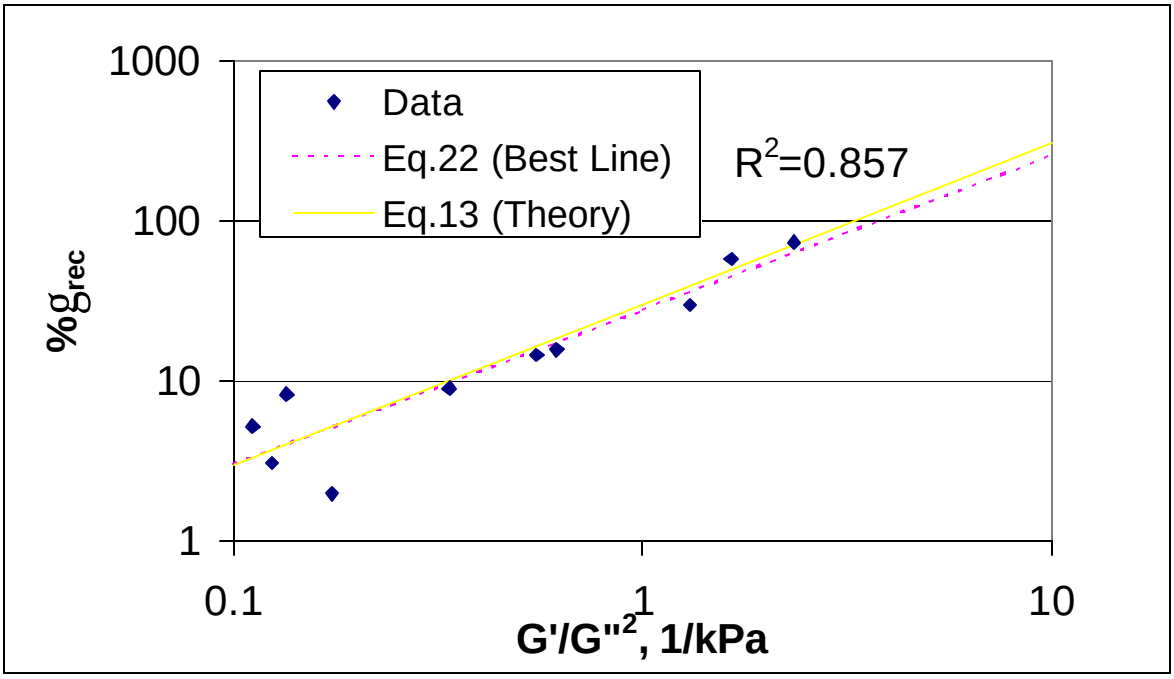

Figure 2: Plot of the percent recoverable strain for an applied stress of 0.3 kPa during creep loading versus the term GN/G0^2 using values obtained from the frequency sweep at matching time scales and temperature.

Figure 2 shows a plot of the percent recoverable strain for an applied stress of 0.3 kPa during creep loading versus the term G''/G'^2 using values obtained from the frequency sweep. Again, the values of the dynamic material functions are chosen at the matching conditions of time scales and temperature. In doing so, the best line through the data points could be fitted with the following equation, which has an R^2 of 0.857:

$$\%\gamma_{rec} = 27.6\left(\frac{G'}{G''^2}\right)^{0.96} \quad \text{----------} \quad (24)$$

The correlation is not as good as for equation (23). Equation (24) deviates a little from equation (13), which predicts that the coefficient should have been 30 and the power on the term (G''/G'^2) should have been 1. In Figure 2 the solid line for equation (13) and the dashed line for equation (24) shows the difference between predictions from theory and the empirical fit. It is not surprising that there is a deviation between equation (13) and equation (24). The elastic component of the material function is normally prone to measurement errors. This is because the memory of the viscoelastic material forces it to remember the deformation that it underwent in the recent past. Thus, unless all the residual stresses are completely relaxed, the measurement of the elastic component of the material function would always be masked by the previous history of its deformation.

Figure 3: Plot of the unrecoverable strain to maximum strain ratio during creep loading versus the phase angle δ obtained from the frequency sweep at matching time scales and temperature.

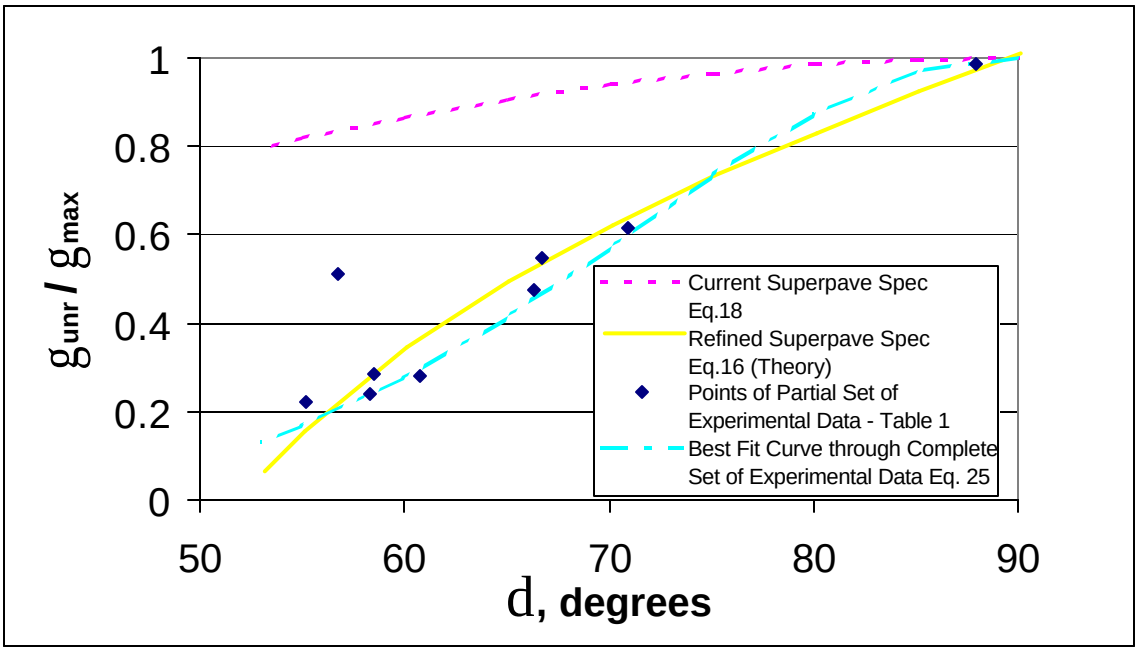

Figure 3 shows the plot of the ratio of unrecoverable strain to maximum strain for an applied stress of 0.3 kPa during creep loading versus the phase angle δ obtained from the frequency sweep. Again, the values of the phase angles are chosen at the matching conditions of time scales and temperature. The solid line is the plot of equation (16) derived from basic principles and gives the predictions based on the refined Superpave specification as given by the expression (20). If the current Superpave specification parameter |G*| / sin δ is used in its place, then the ratio of the unrecoverable strain to maximum strain is predictable through the variation of sin δ as given by equation (18). The dashed line in Figure 3 shows the predictions based on the current Superpave specification. It can be seen that the theoretical predictions from the refinement match the points from the partial set of actual experimental data much better than those when current Superpave specification is used. There are a few noticeable outliers. These are the points corresponding to those that deviated in Figure 2 as well. The reason for this deviation is dependent on the possible measurement errors of the elastic component of the material function as explained earlier.

For viscoelastic materials, it is the ratio of the relaxation time to the process time (or deformation time) to which the material is subjected that controls the material response. An effort was made to match the time scales of shear that takes place during the creep test with that during the frequency sweep by using $\omega = 1/t$. However, this may not be enough since the frequency ω gives the number of radians per second of the oscillations but does not tell how long the material was sheared under these oscillations before the measurement was taken. The measuring time duration t_m at the relevant frequency should, in principle, be also matched and that would reduce the scatter of data in the plots. This was not done in the present case, since it is not easy to do within the sensitivity range of the measuring equipment. For example, for time of applied stress during creep of t = 1 second, the frequency $\omega = 1$ radians/s was used but the measuring time duration t_m was 30 seconds instead of 1 second. The frequency sweep data at $t_m = 1$ second is outside the instrument capability. One option is to obtain the frequency sweep data at various measuring time durations from 30 seconds downwards and extrapolate the values of $|G^*|$ and δ for $t_m = 1$ second. The other option is to obtain frequency sweep data at a value of t_m as close to 1 second as is allowed within the capability of the instrument and use the values of $|G^*|$ and δ for that t_m as an approximation. In either case, the accuracy of the experimental verification of the theoretical development will improve.

After the initial verification through the partial set of data, the complete set of experimental data of Bouldin et al. (2001) was then considered in order to establish authenticity. The best-fit curve through the entire set was found to be mapped by the following equation:

$$\frac{\%g_{unr}}{\%g_{\max}} = (\sin d)^P \quad \text{----------} \quad (25)$$

where P = 9 gave the best fit through the complete set of experimental data. The solid-dashed line in Figure 3 shows the best-fit curve and it can be seen that this follows the predictions of the theoretical equation (16) rather closely, thereby rendering authenticity to the theoretical development.

Equation (19) gives the unrecovered strain per cycle for applied stress F_0. To obtain the accumulated strain, it is necessary to carry out a summation over the number of cycles as

follows. In actual practice, neither the magnitude of the applied stress nor the duration of the stress or the temperature at which the stress is applied may be constant. Hence, the expression for the accumulated strain is written in the most general form as follows:

$$\%g_{acc} = \sum_{i=1}^{N} \frac{100 s_{0i}}{|G^*|(w_i, T_i)} \left(1 - \frac{1}{\tan d(w_i, T_i) \sin d(w_i, T_i)} \right) - - - - - (26)$$

If the magnitude of the applied stress, the duration of the stress and the temperature are constant, then $\%\gamma_{acc} = N\ \%\gamma_{unr}$, and the plot of $\%\gamma_{acc}$ versus number of cycles (or time) is a straight line with a slope given by the right-hand side of equation (19). Equation (26), however, gives an opportunity to input values corresponding to different loading levels, different traffic speeds, and different pavement temperatures for each duration of loading.

The entire development in this paper is general in nature and should be applicable to mastics and mixtures as well. In the case of mastics, since the data is generated on the DSR similar to that for the binder, the procedure for verification of the efficacy of the proposed equation is exactly the same. On the other hand, for aggregate-asphalt mixtures, the data is generated on the Superpave shear tester (SST). If the creep loading and recovery tests are performed on aggregate-asphalt mixtures, then the resulting data would correlate with the results from frequency sweep constant height (FSCH) data performed on the Superpave shear tester (SST) in accordance with the equations set up in this paper on account of the generality of the derivation. However, it must be borne in mind that the suggested equation is not valid at phase angles below 52 degrees. This will naturally restrict the use of this equation to only limited temperature ranges for every aggregate-asphalt mixture set, since in the case of mixtures the phase angles are more likely to be below 52 degrees than above it in the conventional test temperature ranges. As an alternative, in the case of aggregate-asphalt mixtures, one could use equation (25) as a reasonable approximation since this equation closely follows the predictions of equation (16) and at the same time, can be applied to the entire range of phase angles from 90 to 0 degrees. This implies that the term $|G^*|/(\sin \delta)^P$ with P = 9 may be used as a new specification parameter for aggregate-asphalt mixtures for assessing the rutting potential of mixes. The value of P = 9 was obtained by best curve-fitting of binder data alone and hence may be changed in the case of mixes to another value if a better correlation is obtained. It should be noted that, in all fairness, rutting behavior cannot be predicted and arrested by only testing the binder, since it is in fact more of a reflection of the property of the mix.

Acknowledgements

The author wishes to express his gratitude to Dr. Raj Dongré and Mr. Satish Ramaiah for providing the experimental data that was used for verification of the theoretical development in this paper. This was part of the same data that was used by Bouldin et al. (2001) in their paper. The author is grateful to Dr. Ernest J. Bastian, Jr. and Mr. Kevin D. Stuart for their valuable comments.

APPENDIX. REFERENCES

American Association of State Highway and Transportation Officials (2000). "Method for determining the rheological properties of asphalt binder using a Dynamic Shear Rheometer (DSR)." AASHTO Provisonal Standard Designation TP5-98: Washington D. C.

Bahia, H. U., Zeng, M., Zhai, H. and Khatri, A. (1999). "Superpave protocols for modified asphalt binders", Fifteenth quarterly progress report for NCHRP Project 9-10: Washington D.C.

Bird, R. B., Armstrong, R. C. and Hassager, O. (1977). Dynamics of Polymeric Liquids Vol. 1: Fluid Mechanics. John Wiley & Sons, New York.

Bouldin, M. G., Dongré, R., Zanzotto, L. and Rowe, G. M. (2000). "The application of visco-elastic models to predict the relative performance of binders for grading purposes", Proceedings of 2nd Eurasphalt & Eurobitume Congress, Barcelona, Spain, Book 1, 74-82.

Bouldin, M. G., Dongré, R. and D'Angelo, J. (2001). "Proposed refinement to the Superpave high temperature specification parameter for performance graded binders", Presented at the 80th Annual Meeting of the Transportation Research Board, Washington D. C.

Desmazes, C., Lecomte, M., Lesueur, D. and Phillips, M. (2000). "A protocol for reliable measurement of zero-shear-viscosity in order to evaluate the anti-rutting performance of binders", Proceedings of 2nd Eurasphalt & Eurobitume Congress, Barcelona, Spain, Book 1, 202-211.

Phillips, M. C. and Robertus, C. (1996). "Binder rheology and asphaltic pavement permanent deformation; the zero-shear viscosity", Presented at the Eurasphalt & Eurobitume Congress.

Plazek, D. J. and Frund, Z. N. (2000). "Recoverable creep compliance properties and associative model polymer and polyoxyethylene solutions", J. Rheol. **44**, 929-946.

Shenoy, A. V. and Saini, D. R. (1996). Thermoplastic Melt Rheology and Processing. Marcel Dekker Inc., New York

Stuart, K. D. and Mogawer, W. S. (1997). "Validation of asphalt binder and mixture tests that predict rutting susceptibility using FHWA Accelerated Loading Facility", Proc. AAPT **66**: 109-152.

APPENDIX. NOTATION

a,b,c	model parameters in Eq. (3b) as given by Bouldin et al. (2001)
C	arbitrary adjustable constant in the Spriggs model in Eq. (10) and (11)
f(δ)	function of phase angle δ as given by Bouldin et al. (2001)
|G*|, G′, G″	complex shear modulus, dynamic storage modulus, dynamic loss modulus (kPa)
i	index indicating the cycle number in Eq. (23)
J(t)	shear creep compliance (1/kPa)
J_d	delayed recoverable shear compliance (1/kPa)
J_e	elastic recoverable shear compliance (1/kPa)
$J_r(t)$	recoverable shear creep compliance (1/kPa)
$J_{rec}(t)$	steady-state recoverable creep compliance (1/kPa)
k, k_1, k_2	constants in Eq. (3) as given by Bouldin et al. (2000, 2001)
N	number of cycles in Eq. (23)
R	rutting resistance in Eq. (1)
t	time (s)
T	temperature (degrees)
$T_{hi,spec}$	high specification temperature (degrees)
X_0,Y_0	model parameters in Eq. (3b) as given by Bouldin et al. (2001)
δ	phase angle(degrees or radians)
γ_{max}	maximum strain (or total deformation)
γ_{rec}	recoverable strain
γ_{unr}	unrecovered (or permanent) strain
u	shear rate (/s)
η	steady-state shear viscosity (kPa.s)
F_0	applied stress during creep loading (kPa)
τ_{12}	shear stress (kPa)
$\tau_{11} - \tau_{22}$	primary normal stress difference (kPa)
R(t)	normalized retardation function
ω	frequency of oscillatory motion (radians/s)
ω_{spec}	frequency of oscillatory motion (radians/s)